

# Journal of Materials Science

## Heat capacity, thermal expansion and barocaloric effect in fluoride K<sub>2</sub>TaF<sub>7</sub>

--Manuscript Draft--

<b>Manuscript Number:</b>			
<b>Full Title:</b>	Heat capacity, thermal expansion and barocaloric effect in fluoride K <sub>2</sub> TaF <sub>7</sub>		
<b>Article Type:</b>	Manuscript (Regular Article)		
<b>Keywords:</b>	phase transition, heat capacity, entropy, thermal expansion, barocaloric effect		
<b>Corresponding Author:</b>	Igor Flerov Institut fiziki imeni Kirenskogo SO RAN Krasnoyarsk, RUSSIAN FEDERATION		
<b>Corresponding Author Secondary Information:</b>			
<b>Corresponding Author's Institution:</b>	Institut fiziki imeni Kirenskogo SO RAN		
<b>Corresponding Author's Secondary Institution:</b>			
<b>First Author:</b>	Igor Flerov		
<b>First Author Secondary Information:</b>			
<b>Order of Authors:</b>	Igor Flerov Mikhail Gorev Andrey Kartashev Evgeny Pogoreltsev Nataly Laptash		
<b>Order of Authors Secondary Information:</b>			
<b>Abstract:</b>	Heat capacity and thermal dilatation of potassium heptafluorotantalate were studied. Room temperature phase P21/c is stable at least to 4 K. Strong first order phase transition P21/c ↔ Pnma at T <sub>0</sub> = 486.2 K is accompanied by giant changes in the entropy, $\Delta S_0 = 22.3$ J/mol·K, and volume strain, $\delta V_0/V = -3.5\%$ . A rather high sensitivity of K <sub>2</sub> TaF <sub>7</sub> to pressure was found, $dT_0/dp = -220$ K/GPa. Significant extensive and intensive barocaloric effects are found at low pressure. The possibility of improving the barocaloric properties is discussed.		
<b>Funding Information:</b>	<table border="1"><tr><td>Российский Фонд Фундаментальных Исследований (РФФИ) (18 - 02 - 00269a)</td><td>Prof. Igor Flerov</td></tr></table>	Российский Фонд Фундаментальных Исследований (РФФИ) (18 - 02 - 00269a)	Prof. Igor Flerov
Российский Фонд Фундаментальных Исследований (РФФИ) (18 - 02 - 00269a)	Prof. Igor Flerov		

Dear Editor,

Consider please our manuscript, devoted to some new results obtained during the study of heat capacity, thermal dilatation and intensive and extensive barocaloric effects near phase transitions in proper ferroelastic  $K_2TaF_7$ .

We hope that the results will be of interest to readers of Journal of Materials Science.

Sincerely Yours,

Prof. Igor Flerov

### **Heat capacity, thermal expansion and barocaloric effect in fluoride $K_2TaF_7$**

I. N. Flerov, M. V. Gorev, A. V. Kartashev, E. I. Pogoreltsev,  
N.M. Laptash

#### Abstract

Heat capacity and thermal dilatation of potassium heptafluorotantalate were studied. Room temperature phase  $P2_1/c$  is stable at least to 4 K. Strong first order phase transition  $P2_1/c \leftrightarrow Pnma$  at  $T_0 = 486.2$  K is accompanied by giant changes in the entropy,  $\Delta S_0 = 22.3$  J/mol·K, and volume strain,  $\delta V_0/V = -3.5\%$ . A rather high sensitivity of  $K_2TaF_7$  to pressure was found,  $dT_0/dp = -220$  K/GPa. Significant extensive and intensive barocaloric effects are found at low pressure. The possibility of improving the barocaloric properties is discussed.

## Heat capacity, thermal expansion and barocaloric effect in fluoride $K_2TaF_7$

I. N. Flerov<sup>1,2,\*</sup> · M. V. Gorev<sup>1,2</sup> ·  
A. V. Kartashev<sup>1,3</sup> · E. I. Pogorel'tsev<sup>1,2</sup> ·  
N. M. Laptash<sup>4</sup>

Received: date / Accepted: date

**Abstract** Heat capacity and thermal dilatation of potassium heptafluorotantalate were studied. Room temperature phase  $P2_1/c$  is stable at least to 4 K. Strong first order phase transition  $P2_1/c - Pnma$  at  $T_0 = 486.2$  K is accompanied by giant changes in the entropy,  $\Delta S_0 = 22.3 \text{ J} \cdot (\text{mol} \cdot \text{K})^{-1}$ , and volume strain,  $\delta V_0/V = -3.6\%$ . A rather high sensitivity of  $K_2TaF_7$  to pressure was found,  $dT_0/dp = -220 \text{ K G} \cdot \text{Pa}^{-1}$ . Significant extensive and intensive barocaloric effects are found at low pressure. The possibility of improving the barocaloric properties is discussed.

**Keywords** Phase transition · Heat capacity · Entropy · Thermal expansion · Barocaloric effect

### Introduction

The shape of the anionic polyhedron in complex inorganic fluorides can be rather different depending on the valency and size of the central atom, and plays an important role in the formation of crystal lattice and physical properties of compounds [1]. Octahedral anions  $MF_6^{m-}$  are the most frequent structural building units. However, there are also many compounds with other form of fluorine polyhedron. For example, the structure of fluorides with the general chemical formula  $A_2MeF_7$  consists of the seven-coordinated  $MeF_7^{2-}$  anionic complex in the form of mono-capped trigonal prism with  $C_{2v}$  symmetry [2]. Heptafluorides  $A_2TaF_7$  (A: K,  $NH_4$ , Rb) belonging to this series of crystals are characterized by different room temperature symmetry of the crystal lattice depending on the size of the monovalent cation A. While compounds with  $A = Rb, NH_4$  have tetragonal

<sup>1</sup>Kirensky Institute of Physics, Federal Research Center KSC Siberian Branch, Russian Academy of Sciences, Krasnoyarsk, 660036 Russia

<sup>2</sup>Institute of Engineering Physics and Radioelectronics, Siberian State University, 660074 Krasnoyarsk, Russia

<sup>3</sup>Astafijev Krasnoyarsk State Pedagogical University, 660049 Krasnoyarsk, Russia

<sup>4</sup>Institute of Chemistry, Far East Branch, Russian Academy of Sciences, Vladivostok, 690022 Russia

\* Address correspondence to E-mail: flerov@iph.krasn.ru

1 symmetry ( $P4/nmm$ ,  $Z = 2$ ) [3], potassium heptafluorotantalate is monoclinic  
 2 ( $P2_1/c$ ,  $Z = 4$ ) [2,4]. Crystal lattice stability of heptafluorides with respect to  
 3 temperature change is also different. The tetragonal phase of the first two crystals  
 4 is stable when heated to the decomposition temperature. Upon cooling, both com-  
 5 pounds undergo unique and successive phase transitions:  $\text{Rb}_2\text{TaF}_7 - P4/nmm$   
 6 ( $T_0 = 145$  K) -  $Cmma$  [5];  $(\text{NH}_4)_2\text{TaF}_7 - P4/nmm$  ( $T_1 = 174$  K) -  $Pmnm$   
 7 ( $T_2 = 156$  K) - tetragonal [6]. In accordance with small values of the correspond-  
 8 ing entropy change ( $\Delta S \leq 0.5R$ ), all of these transformations were considered as  
 9 belonging to the displacive type [5,6].

10 Monoclinic phase in  $\text{K}_2\text{TaF}_7$  remains stable when cooled to at least 100 K [7]  
 11 and, upon heating, potassium heptafluorotantalate undergoes two structural phase  
 12 transitions [8]. One of them takes place at 998 K which is very close to the point  
 13 of the incongruent melting at 1022 K and accompanied by the mass loss. This is  
 14 the reason why the main attention of investigators is usually paid to the reverses  
 15 structural transformation  $P2_1/c$  ( $T_0 = 475$  K) -  $Pnma$  ( $Z=4$ ) [4] which is rather  
 16 unusual in respect to the following intriguing points. (1) Space groups  $P2_1/c$  and  
 17  $Pnma$  are connected by the group-subgroup relation, however, the large structural  
 18 distortions in monoclinic phase and huge thermal hysteresis were found [8] which  
 19 are typical for reconstructive phase transition. (2) Despite the absence of struc-  
 20 tural disorder in phase  $Pnma$  [9], large entropy change,  $\Delta S = R \ln 6$ , obtained  
 21 using differential scanning calorimeter (DSC), is characteristic for order-disorder  
 22 transformation [8]. This contradiction can be explained taking into account a giant  
 23 change in the volume of the anionic polyhedron as well as the coordination number  
 24 of the central atom Ta. (3) The origin of structural distortions was characterized  
 25 as "proper" ferroelastic and a significant change in the phase transition parameter  
 26  $\eta$  was found in a wide range of temperatures below  $T_0$ . But the temperature de-  
 27 pendent part of the corresponding entropy  $\Delta S(T) \sim \eta^2(T)$  was detected in DSC  
 28 measurements only in rather narrow temperature region [8]. (4) Heat treatment  
 29 causes changes in the temperature and enthalpy of the phase transition, but does  
 30 not change the corresponding entropy [7].

31 Due to a large change in entropy during the phase transition, it is possible  
 32 to assume a very high barocaloric efficiency of  $\text{K}_2\text{TaF}_7$ . However, to analyze the  
 33 intensive and extensive barocaloric effects (BCE), detailed information is needed  
 34 on the temperature dependencies of entropy and elastic deformation, as well as on  
 35 the sensitivity of the temperature of the phase transition to external pressure.  
 36

37 In the present paper, we carried out thorough studies of the heat capacity and  
 38 thermal expansion in a wide temperature range which allowed one to determine  
 39 the main thermodynamic parameters of the phase transition  $P2_1/c - Pnma$ . We  
 40 also evaluated the baric coefficient,  $dT_0/dp$ , characterizing stability of the crystal  
 41 lattice in respect to hydrostatic pressure as well as intensive  $\Delta T_{AD}$  and extensive  
 42  $\Delta S_{BCE}$  BCE.  
 43  
 44

## 45 Sample preparation and measurement technique

### 46 Sample preparation and characterization

47 Potassium heptafluorotantalate was prepared by its precipitation from hydroflu-  
 48 oric acid solution. A starting material,  $\text{Ta}_2\text{O}_5$ , of a reagent grade was dissolved  
 49  
 50  
 51  
 52  
 53  
 54  
 55  
 56  
 57  
 58  
 59  
 60  
 61  
 62  
 63  
 64  
 65

1 in concentrated HF (40% wt) at heating followed by addition of KCl. A stoichiometric  
2 quantity of potassium salt was added to the solution diluted with water. In  
3 accordance with the reaction:  $\text{H}_2\text{TaF}_7 + 2\text{KCl} = \text{K}_2\text{TaF}_7 + 2\text{HCl}$ . The crystalline precipitate  
4 was filtered of and washed under vacuum with alcohol. Using EDX and  
5 XPS methods, the composition of the crystals was checked. Both indicated the  
6 oxygen presence. The fluorine amount was determined by a fluoride ion-selective  
7 electrode calibrated with different diluted solutions of standard NaF. The real content  
8 of fluorine was  $31.5 \pm 0.4\%$  (compared to the calculated 33.92% for  $\text{K}_2\text{TaF}_7$ ).  
9 Thus, the composition of the crystals grown is  $\text{K}_2\text{TaO}_{0.3}\text{F}_{6.4}$ .

10 X-ray studies were performed to make sure that such an amount of oxygen  
11 impurity does not affect the type of structure. All peaks on the powder diffraction  
12 patterns were indexed by monoclinic cell  $P2_1/c$  with parameters close to  
13 previously found for  $\text{K}_2\text{TaF}_7$  [2,10]. This crystal structure was taken as starting  
14 model for Rietveld refinement which was found to be stable revealing low  $R$ -factors  
15 ( $R_{wp}=5.81\%$ ,  $R_p=4.64\%$ ,  $\chi^2=1.63$ ). Thus, we can use the stoichiometric formula  
16  $\text{K}_2\text{TaF}_7$ .  
17

### 18 Dilatometry

19 Measuring the thermal expansion was performed using a push-rod dilatometer  
20 (NETZSCH model DIL-402C) with a fused silica sample holder. Experiments were  
21 carried out in the temperature range of 100–750 K with a heating rate of  $3 \text{ K}\cdot\text{min}^{-1}$   
22 in a dry He flux. The results were calibrated, by taking quartz as the standard  
23 reference in order to eliminate the influence of thermal expansion of the system.  
24 The reproducibility of data obtained in all successive series of measurements was  
25 not less than 5%. Samples for dilatometric measurements were prepared as quasi-  
26 ceramic disc-shaped pellets of 6 mm diameter and 1.3 mm thickness.  
27  
28  
29

### 30 Calorimetry

31 Detailed measurements of heat capacity,  $C_p(T)$ , of  $\text{K}_2\text{TaF}_7$  were performed in a  
32 wide temperature range of 4–600 K by means of three calorimetric methods.  
33

34 Below 90 K, the dependence  $C_p(T)$  was studied using a special option of a  
35 Physical Property Measurement System (PPMS, Quantum Design, USA). Measurements  
36 were performed on a ceramic sample. Apiezon N grease was used to provide reliable  
37 thermal contact between the sample and the additives. The relative error of measurements  
38 was less than 1%.  
39

40 A homemade adiabatic calorimeter with three screens, as described in Ref. [11],  
41 was used in experiments between 80 and 320 K. The heat capacity of the "sample +  
42 heater + contact grease" system was measured using discrete as well as continuous  
43 heating. In the former case, the temperature step was varied from 1.5 to 3.0 K.  
44 In the latter case, the system was heated at rates of about  $0.15\text{--}0.30 \text{ K}\cdot\text{min}^{-1}$ .  
45 The heat capacities of the heater and contact grease were determined in individual  
46 experiments. The inaccuracy in the heat capacity determination did not exceed  
47 0.5–1.0%.  
48

49 The high-temperature heat capacity was measured by DSC on a NETZSCH 204  
50 F1 instrument in a dry helium flow ( $20 \text{ ml}\cdot\text{min}^{-1}$ ) in the 300–600 K temperature  
51  
52  
53  
54  
55  
56  
57  
58  
59  
60  
61  
62  
63  
64  
65

range at a heating rate of  $5 \text{ K}\cdot\text{min}^{-1}$  with the accuracy  $\sim 2\%$ . Sapphire was used as the standard.

## Results and discussion

### Thermal dilatation

Results of two consecutive dilatometric experiments are presented in Fig. 1. In the first heating mode measurements were started from 100 K. Temperature behavior of the coefficient of volume thermal expansion,  $\beta$ , and volumetric strain,  $\Delta V/V = 3(\Delta L/L)$ , shows only one anomaly at  $T_0 = 486 \pm 1 \text{ K}$ . According to very large value of the thermal hysteresis  $\delta T_0 \approx 50 \text{ K}$  [8], the phase transition should take place upon cooling at 436 K. Due to the specific features of the dilatometric installation, measurements in the cooling mode can be carried out only down to  $\sim 450 \text{ K}$  and as a result no anomalies were detected upon cooling. During the second heating, started from 300 K, a more pronounced negative anomaly  $\Delta\beta$  was observed, which is about two times larger than the anomaly during the first heating. The observed difference may be due to the residual mechanical stresses arising in the quasi-ceramic sample during its preparation and their annealing during the first heating to 750 K.

In accordance with the first order  $Pnma-P2_1/c$  transformation, strong anomalous behavior in the volume strain was observed in the narrow temperature range around  $T_0$  with the negative strain jump  $\delta V_0/V = -(36 \pm 5) \times 10^{-3}$  (Fig. 1(b)). This value gives the dominant contribution to the total change in the volume strain and clearly indicates that the phase transition is far from the tricritical point where  $\delta V_0/V \rightarrow 0$ .

### Heat capacity

Good agreement was found between the results of calorimetric measurements performed by three different methods. The behavior of the molar heat capacity in the entire temperature range studied is shown in Fig. 2(a) and demonstrates, firstly, the stability of the monoclinic phase  $P2_1/c$  to very low temperature (4 K), and, secondly, the existence of only one strongly asymmetric heat capacity anomaly above room temperature corresponding to the  $Pnma - P2_1/c$  phase transition. The temperature of the  $C_p(T)$  maximum,  $T_0 = 486.2 \pm 0.5 \text{ K}$ , agrees well with the value of the phase transition temperature found in dilatometric measurements and turned out to be slightly lower than  $T_0$  observed in optical experiments on single crystals (503–508 K) [7]. To determine the hysteresis value  $\delta T_0$  in the sample under study, we performed measurements using DSC. Fig. 3 shows the temperature dependence of DSC signal measured in heating and cooling modes. At thermal cycling rate equal to  $dT/dt = 5 \text{ K}\cdot\text{min}^{-1}$ , the DSC peaks corresponded to phase transition temperature were found at  $484.5 \pm 1 \text{ K}$  and  $447.5 \pm 1 \text{ K}$  upon heating and cooling, respectively. The observed value  $\delta T_0 \approx 37 \text{ K}$  shows why a structural transformation was not detected in dilatometric experiments during the cooling process.

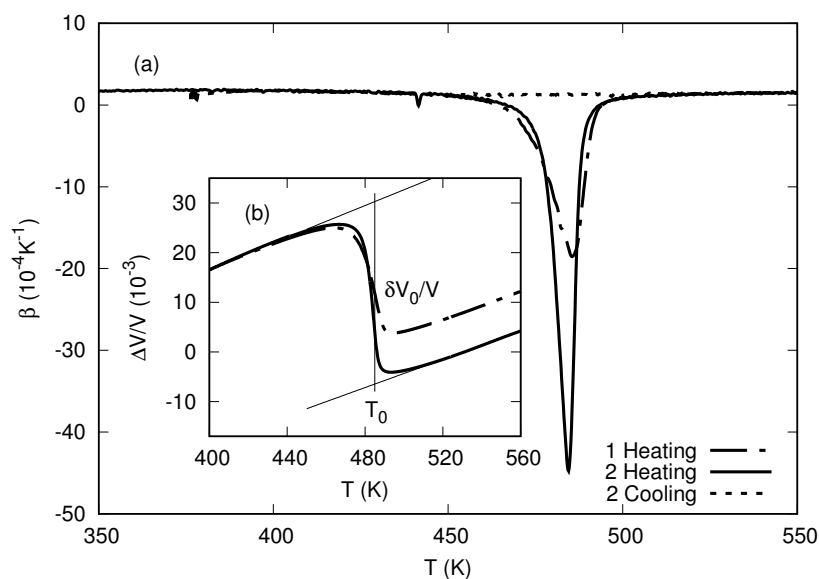


**Fig. 1** Temperature dependencies of thermal expansion coefficients  $\beta$  (a) and the volume strains  $\Delta V/V$  (b) of  $K_2TaF_7$ . Dashed line is lattice contribution  $\beta_L(T)$  that coincides with the behavior of  $\beta(T)$  measured in cooling mode

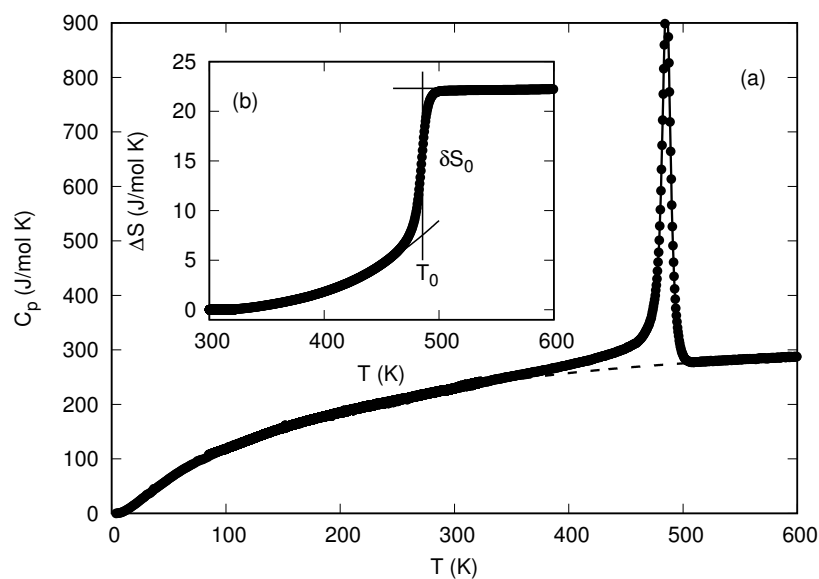


**Fig. 2** Temperature dependencies of the molar heat capacity (a) and anomalous entropy (b) of  $K_2TaF_7$ . Dashed line corresponds to the lattice heat capacity  $C_L$

To get information about the entropy of the phase transition, it was necessary to separate the anomalous,  $\Delta C_p$ , and lattice,  $C_L$ , contributions to the total heat capacity,  $C_p$ , of  $K_2TaF_7$ .

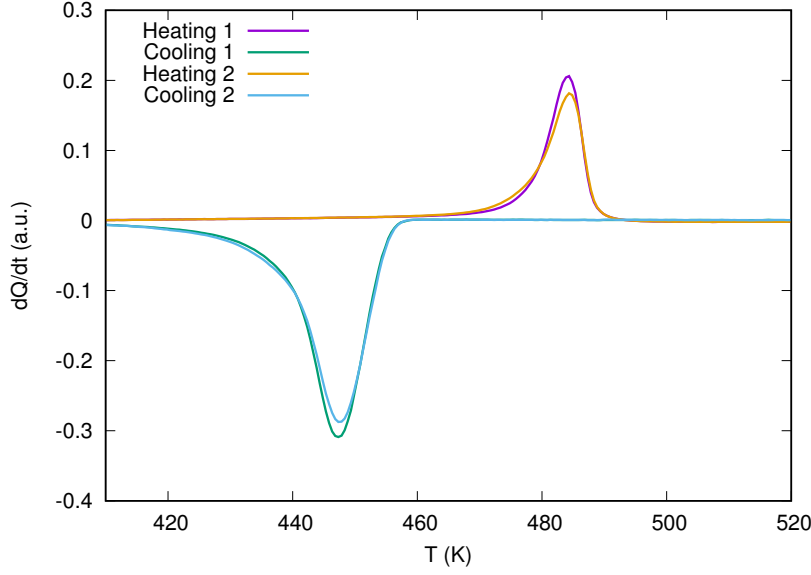


**Fig. 3** Temperature dependencies of  $dQ/dt$  measured in DSC experiments upon heating and cooling at the rate  $5 \text{ K}\cdot\text{min}^{-1}$

This procedure was carried out using a simple model describing  $C_L(T)$ . The experimental data taken far from the transition points ( $T < 300 \text{ K}$  and  $T > 510 \text{ K}$ ) were fitted using a linear combination of Debye and Einstein terms  $C_L = K_D C_D + K_E C_E$ , where

$$C_D(T) = 9R \left( \frac{T}{\Theta_D} \right)^3 \int_0^{\Theta_D/T} \frac{x^4 \exp(x)}{(\exp(x) - 1)^2} dx, \quad (1)$$

$$C_E(T) = 3R \left( \frac{\Theta_E}{T} \right)^2 \frac{\exp(\Theta_E/T)}{(\exp(\Theta_E/T) - 1)^2} \quad (2)$$

and  $K_D$ ,  $K_E$ ,  $\Theta_D$ ,  $\Theta_E$  are fitting parameters.

The average deviation of the experimental data from the smoothed curve does not exceed 1%. The lattice contribution is shown by a dashed line in Fig. 2(a). The anomalous heat capacity,  $\Delta C_p = C_p - C_L$ , was observed in very wide temperature range below the phase transition point  $T_0 - 140 \text{ K}$  which correlates with the behavior of the phase transition parameter [7].

Fig. 2(b) demonstrates the temperature behavior of excess entropy associated with the phase transitions in  $\text{K}_2\text{TaF}_7$ , determined by integration of the area under the  $\Delta C_p$  versus  $T$  curve:  $\Delta S_0 = 22.3 \pm 2.0 \text{ J}\cdot(\text{mol}\cdot\text{K})^{-1}$ . The entropy jump associated with the first order phase transition was estimated to be equal approximately  $\delta S_0 = 14.5 \pm 2.0 \text{ J}\cdot(\text{mol}\cdot\text{K})^{-1}$  (Fig. 2(b)).

Significant changes in entropy ( $\Delta S_0 \approx R \ln 16$ ) and cell volume ( $\delta V_0/V \approx 3.6 \%$ ) during phase transformation indicate that the distortions of the structure can be associated with the order-disorder processes. However, analysis of structural data [9] showed that in the high-temperature phase there is no disordering



of any structural elements, the ordering of which could lead to an order–disorder transition. At the same time, in the  $P2_1/c$  phase, the displacements of all atoms turned out to be anomalously large.

It can be assumed that the cause of anomalously large entropy can be, firstly, a pronounced (but not extreme, leading to disordering) anharmonicity of atomic vibrations in the  $Pnma$  phase, and secondly, the reconstructive nature of the transition accompanied by a giant jump in volume. It should be noted, however, that this is an unusual reconstructive transition, since the symmetries of the high-temperature and low-temperature phases are related by the group–subgroup relation.

Thus, the mechanism of the phase transition in  $\text{K}_2\text{TaF}_7$  is very complex and remains uncertain to date.

#### Effect of hydrostatic pressure

Calorimetric and dilatometric studies have provided reliable evidence of the first order of phase transition in  $\text{K}_2\text{TaF}_7$ . The susceptibility of transformations of this kind to hydrostatic pressure can be determined within the framework of the Clausius–Clapeyron equation, using the heat capacity and thermal dilatation data

$$\frac{dT_0}{dp} = \frac{\delta V_0}{\delta S_0} = V_m \frac{\delta V_0/V}{\delta S_0}, \quad (3)$$

where  $V_m$  – molar volume and  $\delta S_0$ ,  $\delta V_0$  are entropy and volume jumps at  $T_0$ , respectively. Estimation of the derivative of the transition temperature with respect to pressure gives the value  $dT_0/dp \approx -220 \pm 20 \text{ K}\cdot\text{GPa}^{-1}$ .

To more correctly determine the magnitude of the baric coefficient, one can use the Pippard relation, which relates the temperature dependencies of the thermal expansion coefficient and heat capacity in the vicinity of the phase transition

$$C_p = \frac{V_m T_0}{\gamma} \beta + \text{const}, \quad \gamma = \frac{dT_0}{dp}. \quad (4)$$

Because the value of  $dT_0/dp$  is strongly depend on the data close to the phase transition point, small errors in temperature scales of measurements of heat capacity (temperature sensor – platinum thermometer) and thermal expansion (temperature sensor – thermocouple) will lead to significant errors in the results obtained using the Pippard relation. In this regard, the data on the thermal expansion and heat capacity were reduced to one temperature scale by alignment of the phase transition temperatures.

The results of joint analysis of dependencies of  $C_p(T)$  and  $\beta(T)$  below  $T_0$  are shown in Fig. 4. The experimental points fall on a straight line which means that the Pippard relation is fairly satisfied in rather wide temperature range  $T_0 - T = (5-35) \text{ K}$ . Deviations from linear behavior are observed near  $T_0$ , where the imperfections of the sample, the dynamic mode of the thermal expansion measurements, and the difference in temperature scales for  $C_p(T)$  and  $\beta(T)$  measurements play a significant role. The obtained value of the baric coefficient  $dT_0/dp \approx -212 \pm 15 \text{ K}\cdot\text{GPa}^{-1}$  agrees well with that calculated from the Clausius–Clapeyron equation and gives us hope that the value of  $dT_0/dp$  is close to real one as well.

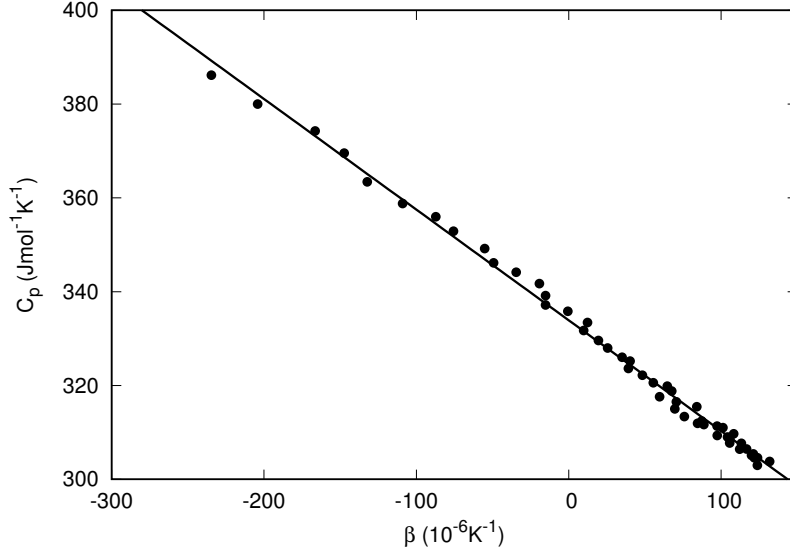


**Fig. 4** The relationship between the molar heat capacity and the coefficient of volume thermal expansion below  $T_0$

A negative sign and a large value of  $dT_0/dp$  indicate the possibility of a shift of the  $Pnma - P2_1/c$  phase transition to room temperature under pressure of about 1 GPa. Due to the combination of large values of  $\Delta S_0$  and  $dT_0/dp$ , the barocaloric efficiency of  $K_2TaF_7$  turns out to be very high.

#### Barocaloric effect

Barocaloric effect is associated with the reversible change in entropy,  $\Delta S_{BCE}$ , or temperature,  $\Delta T_{AD}$ , of a thermodynamic system with a change in pressure under isothermal or adiabatic conditions, respectively. An important characteristic of barocaloric efficiency is also a minimum pressure,  $p_{min}$ , required to implement maximum values of the extensive,  $\Delta S_{BCE}^{max}$ , equal to the phase transition entropy, and intensive,  $\Delta T_{AD}^{max}$ , effects. In the case of the strictly first order phase transition, the relations between these three parameters are as follows [12, 13]:

$$p_{min} \geq \frac{T \Delta S_0}{C_L dT_0/dp}, \quad \Delta T_{AD}^{max} \approx \frac{dT_0}{dp} p_{min} \quad (5)$$

Using the values  $C_L$ ,  $\Delta S_0$  and  $dT_0/dp$  determined above for  $K_2TaF_7$ , we have found:  $p_{min} \approx 0.2$  GPa and  $\Delta T_{AD}^{max} \approx -35 \pm 2$  K. The negative sign of the intensive BCE is associated with a decrease in the volume at the phase transition.

The behavior of both intensive and extensive BCE with change in pressure and temperature was analyzed in the framework of the previously described method [14]. For this aim, temperature dependencies of the total entropy under different pressure (Fig. 5(a)) were determined by summation of the lattice entropy  $S_L =$

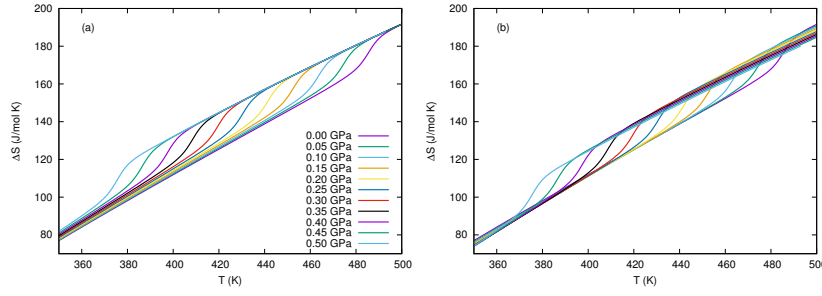


**Fig. 5** Temperature dependencies of total entropy of  $K_2TaF_7$  at different hydrostatic pressure before (a) and after (b) correction for the additional lattice entropy changes with pressure

$\int (C_L/T)dT$  and the anomalous contribution  $\Delta S(T)$  determined at  $p = 0$  and shifted along the temperature scale according to the sign and value of  $dT_0/dp$ .

Recently, studies of differential thermal analysis under pressure for some complex fluorides and oxyfluorides revealed the absence of the pressure effect, at least to 0.6 GPa, on the phase transition entropy [14–16]. Taking into account these results, we assumed that in the case of  $K_2TaF_7$  pressure also does not affect  $\Delta S$ .

The behavior of the extensive BCE determined using temperature and pressure dependencies of the total entropy  $\Delta S_{BCE} = S(T, p) - S(T, p = 0)$  is shown in Fig. 6(a). To obtain correct information on  $\Delta T_{AD}(T, p)$ , plots of  $S(T, p) = S_L(T, p) + \Delta S(T, p)$  were analyzed based on the condition of constant entropy  $S(T, p) = S(T + \Delta T_{AD}, p = 0)$  (Fig. 6(b)).

At the first stage, we did not take into account the changes in the lattice entropy with pressure (Fig. 5(a)). The magnitudes of  $\Delta S_{BCE}$  and  $\Delta T_{AD}$  increase with increasing pressure tending to maximum values but not reaching them at 0.5 GPa which is higher than  $p_{min}$  (Fig. 6(a),(b)). The difference between estimated  $p_{min}$  and experimental pressure is particularly associated with the validity of Eq. 5 for strong first order phase transition whereas  $K_2TaF_7$  undergoes transformation close enough to the tricritical point. Nevertheless, the analysis showed the possibility of realizing very large values of both BCE,  $\Delta S_{BCE} \approx 21 \text{ J} \cdot (\text{mol} \cdot \text{K})^{-1} = 54 \text{ J} \cdot (\text{kg} \cdot \text{K})^{-1}$  and  $\Delta T_{AD} \approx -30 \text{ K}$ , in this crystal at rather low pressure  $p \sim 0.5 \text{ GPa}$ . The intensive BCE is in good agreement with the maximum possible value  $\Delta T_{AD}^{max}$  estimated above. It is necessary to point out, that intensive and extensive BCE found in  $K_2TaF_7$  are comparable and in some cases even exceed barocaloric parameters in other materials [17–20].

On the other hand, the crystal lattice of potassium heptafluorotantalate is characterized by positive volume deformation  $\Delta V_L/V > 0$  and large volumetric thermal expansion coefficient  $\beta_L \approx 1.5 \times 10^{-4} \text{ K}^{-1}$ . In accordance with the Maxwell equation:

$$\left(\frac{\partial S}{\partial p}\right)_T = -\left(\frac{\partial V}{\partial T}\right)_p \quad (6)$$

this peculiarity leads to significant conventional contribution ( $\Delta S_{BCE} < 0$ ,  $\Delta T_{AD} > 0$ ) associated with the crystal lattice expansion to the total BCE and as result decreases the extensive and intensive inverse BCE in the phase transition region.

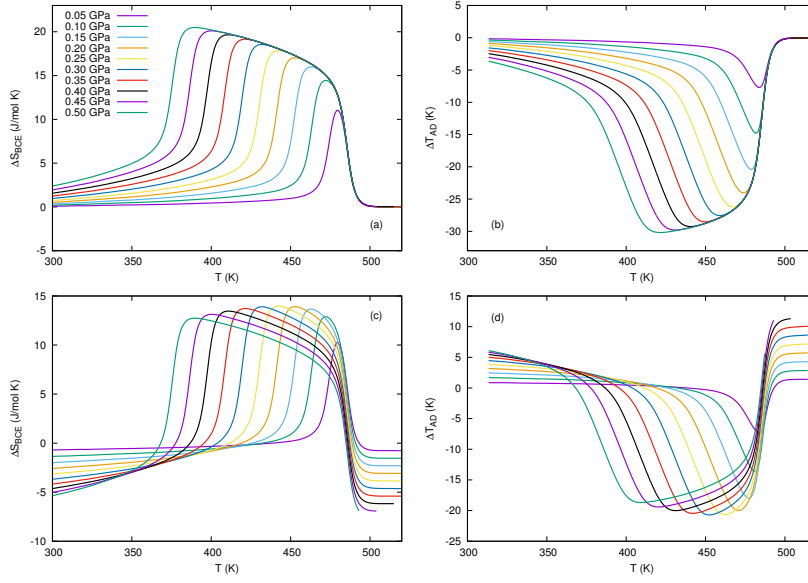


**Fig. 6** Temperature dependencies of barocaloric entropy and temperature changes at different hydrostatic pressure before (a, b) and after (c, d) correction for the additional lattice entropy changes with pressure

Thus, to get detailed and correct information about BCE, it is necessary to know the pressure dependence of the total entropy. Due to a lack of opportunity to measure  $C_p(T, p)$ , the lattice entropy change with pressure,  $\Delta S_L$ , may be expressed using Eq. 6 with  $S$  replacing by  $S_L$

$$\Delta S_L(T, p) = - \int_0^p (\partial V_L / \partial T)_p dp \approx -V_m \beta_L(T) p, \quad (7)$$

We assume here that pressure not significantly affect  $\beta_L$  and  $V_m$ .

Fig. 5(b) shows the temperature dependencies of the total entropy at different pressures taking into account changes in the lattice entropy under pressure. The temperature and pressure dependencies of both the extensive and the intensive BCE determined in this approximation, are shown in Fig. 6 (c) and (d). It can be seen that in this case the behavior of  $\Delta S_{BCE}(T, p)$  and  $\Delta T_{AD}(T, p)$  changed significantly and peak values  $\Delta S_{BCE}^{max}$  and  $\Delta T_{AD}^{max}$  decreased. However, a rather large conventional BCE appeared above the transition temperature. As a result, at  $p = 0.5$  GPa, there are very rapid changes in the values of  $\Delta S_{BCE}$  (from  $-7$  to  $+14 \text{ J} \cdot (\text{mol} \cdot \text{K})^{-1}$  or from  $-18$  to  $+36 \text{ J} \cdot (\text{kg} \cdot \text{K})^{-1}$ ) and  $\Delta T_{AD}$  (from  $+12$  to  $-20$  K). Recently, similar effect of the lattice thermal expansion on BCE was observed in ferroelectric  $(\text{NH}_4)_2\text{SO}_4$  [17].

The phenomenon of a change in the sign of BCE in a narrow temperature range was observed by us earlier in the vicinity of the triple points on the  $T - p$  phase diagrams for a series of fluorides and oxyfluorides [12, 13]. The results obtained in the present paper and [12] are very important and promising from the point of view of searching new materials with large BCE and designing original cooling

cycles. It is obvious that in materials characterized by an increase in the volume of the unit cell during the phase transition and a large value of the positive coefficient of volume thermal expansion far from the transition point, BCE will increase due to the high compliance of the lattice entropy to the pressure.

## Conclusions

Studies of thermal expansion and heat capacity of potassium heptafluorotantalate,  $K_2TaF_7$ , performed in a wide temperature range allowed us to establish the following important points.

Calorimetric measurements showed the stability of the phase  $P2_1/c$  to very low temperature ( $\sim 4$  K). The phase transition  $P2_1/c - Pnma$  ( $Z=4$ ) is a pronounced first order transformation accompanied by large values of thermal hysteresis ( $\delta T_0 \approx 37$  K) and entropy ( $\Delta S_0 = 22.3 \pm 2.0 \text{ J}\cdot(\text{mol}\cdot\text{K})^{-1}$ ) as well as jumps of volume ( $\delta V_0/V = -(3.6 \pm 0.5)\%$ ) and entropy ( $\delta S_0 = 14.5 \pm 2.0 \text{ J}\cdot(\text{mol}\cdot\text{K})^{-1}$ ) at  $T_0=486.2$  K. Anomalous behavior of the heat capacity and entropy is observed in very wide temperature range below the phase transition point  $T_0 - 140$  K which correlates with the behavior of the parameter of the phase transition [7].

A very high sensitivity of the transition temperature to hydrostatic pressure was found. Good agreement is observed between the values  $dT_0/dp$  determined using the Pippard ( $-212 \pm 15 \text{ K}\cdot\text{GPa}^{-1}$ ) and Clausius–Clapeyron ( $-220 \pm 20 \text{ K}\cdot\text{GPa}^{-1}$ ) equations. A large value and a negative sign of the baric coefficient indicate the possibility of a shift of the  $Pnma - P2_1/c$  transformation to room temperature under pressure of about 1 GPa.

Due to the combination of large values of  $\Delta S_0$  and  $dT_0/dp$ ,  $K_2TaF_7$  demonstrates very high barocaloric efficiency. It was shown that large thermal expansion of the crystal lattice leads to large contribution of the conventional BCE to the total effect. The conversion from the conventional BCE to the inverse is observed in narrow temperature range and accompanied by large change of intensive and extensive effects. These results show that barocaloric efficiency can be increased in materials with conventional BCE and large positive value of  $\beta_L$ .

**Acknowledgements** The reported study was funded by RFBR according to the research project No. 18-02-00269\_a.

## Compliance with ethical standards

**Conflict of interest** The authors declare that they have no conflicts of interest.

## References

1. Leblanc M, Maisonneuve V, Tressaud A (2015) Crystal chemistry and selected physical properties of inorganic fluorides and oxide-fluorides. *Chem. Rev.* 115:1191–1254
2. Mazej Z, Hagiwara R (2007) Hexafluoro-, heptafluoro-, and octafluoro-salts, and  $[M_nF_{5n+1}]^-$  ( $n=2, 3, 4$ ) polyfluorometallates of singly charged metal cations,  $Li^+$ ,  $Cs^+$ ,  $Cu^+$ ,  $Ag^+$ ,  $In^+$  and  $Tl^+$ . *J. Fluorine Chem* 128:423 – 437

3. Laptash NM, Udovenko AA, Emelina TB (2011) Dynamic orientation disorder in rubidium fluorotantalate. synchronous Ta–O and Ta–F vibrations. *J. Fluorine Chem.* 132:1152 – 1158
4. Agulyansky A (2003) Potassium fluorotantalate in solid, dissolved and molten conditions. *J. Fluorine Chem.* 123:155 –161
5. Pogorel'tsev E, Mel'nikova S, Kartashev A, Gorev M, Flerov I, Laptash N (2017) Thermal, optical, and dielectric properties of fluoride Rb<sub>2</sub>TaF<sub>7</sub>. *Phys. Solid State* 59:986–991
6. Pogorel'tsev EI, Mel'nikova SV, Kartashev AV, Molokeyev MS, Gorev MV, Flerov IN, Laptash NM (2013) Ferroelastic phase transitions in (NH<sub>4</sub>)<sub>2</sub>TaF<sub>7</sub>. *Phys. Solid State* 55:611–618
7. Mel'nikova SV, Bogdanov EV, Molokeyev MS, Laptash NM, Flerov IN (2019) Optical and calorimetric studies of K<sub>2</sub>TaF<sub>7</sub>. *J. Fluor. Chem.* 222-223:75–80
8. Boča M, Rakhmatullin A, Mlynáriková J, Hadzimová E, Vasková Z, Mičušík M (2016) Differences in XPS and solid state NMR spectral data and thermo-chemical properties of iso-structural compounds in the series KTaF<sub>6</sub>, K<sub>2</sub>TaF<sub>7</sub> and K<sub>3</sub>TaF<sub>8</sub> and KNbF<sub>6</sub>, K<sub>2</sub>NbF<sub>7</sub> and K<sub>3</sub>NbF<sub>8</sub>. *Dalton Trans.* 44:17106–17117
9. Langer V, Smrčok L, Boča M (2006) Dipotassium heptafluorotantalate(V), β-K<sub>2</sub>TaF<sub>7</sub>, at 509 K. *Acta Cryst. E* 62:i91–i93
10. Torardi C, Brixner L, Blasse G (1987) Structure and luminescence of K<sub>2</sub>TaF<sub>7</sub> and K<sub>2</sub>NbF<sub>7</sub>. *J. Solid State Chem* 67:21 – 25
11. Kartashev AV, Flerov IN, Volkov NV, Sablina KA (2008) Adiabatic calorimetric study of the intense magnetocaloric effect and the heat capacity of (La<sub>0.4</sub>Eu<sub>0.6</sub>)<sub>0.7</sub>Pb<sub>0.3</sub>MnO<sub>3</sub>. *Phys. Solid State* 50:2115–2120
12. Gorev M, Bogdanov E, Flerov I (2017) T-p phase diagrams and the barocaloric effect in materials with successive phase transitions. *J. Phys. D: Applied Physics* 50:384002
13. Gorev M, Bogdanov E, Flerov I (2017) Conventional and inverse barocaloric effects around triple points in ferroelastics (NH<sub>4</sub>)<sub>3</sub>NbOF<sub>6</sub> and (NH<sub>4</sub>)<sub>3</sub>TiOF<sub>5</sub>. *Scripta Materialia* 139:53–57
14. Gorev MV, Flerov IN, Bogdanov EV, Voronov VN, Laptash NM (2010) Barocaloric effect near the structural phase transition in the Rb<sub>2</sub>KTiOF<sub>5</sub> oxyfluoride. *Phys. Solid State* 52:377–383
15. Pogorel'tsev E, Flerov I, Kartashev A, Bogdanov E, Laptash N (2014) Heat capacity, entropy, dielectric properties and T–p phase diagram of (NH<sub>4</sub>)<sub>3</sub>TiF<sub>7</sub>. *J. Fluorine Chem* 168:247 – 250
16. Flerov IN, Kartashev AV, Gorev MV, Bogdanov EV, Mel'nikova SV, Molokeyev MS, Pogorel'tsev EI, Laptash NM (2016) Thermal, structural, optical, dielectric and barocaloric properties at ferroelastic phase transition in trigonal (NH<sub>4</sub>)<sub>2</sub>SnF<sub>6</sub>: A new look at the old compound. *J. Fluorine Chem.* 183:1 – 9
17. Lloveras P, Stern-Taulats E, Barrio M, Tamarit JL, Crossley S, Li W, Pomjakushin V, Planes A, Mañosa L, Mathur ND, Moya X (2015) Giant barocaloric effects at low pressure in ferroelectric ammonium sulphate. *Nature Commun* 6:8801
18. Mañosa L, González-Alonso D, Planes A, Bonnot E, Barrio M, Tamarit JL, Aksoy S, Acet M (2010) Giant solid-state barocaloric effect in the Ni-Mn-In magnetic shape-memory alloy. *Nature Mat* 9:478
19. Mañosa L, González-Alonso D, Planes A, Barrio M, Tamarit JL, Titov IS, Acet M, Bhattacharyya A, Majumdar S (2011) Inverse barocaloric effect in the giant magnetocaloric La-Fe-Si-Co compound. *Nature Commun* 2:595
20. Yuce S, Barrio M, Emre B, Stern-Taulats E, Planes A, Tamarit JL, Mudryk Y, Gschneidner KA, Pecharsky VK, Mañosa L (2012) Barocaloric effect in the magnetocaloric prototype Gd<sub>5</sub>Si<sub>2</sub>Ge<sub>2</sub>. *Appl. Phys. Lett.* 101:071906